RSC Advances

PAPER

View Article Online
View Journal | View Issue

Cite this: *RSC Adv.*, 2021, **11**, 678

Facile fabrication and characterization of aliphatic polyketone (PK) micro/nano fiber membranes *via* electrospinning and a post treatment process†

Jian Hou,‡[ab] Chanju Park,‡[b] Wongi Jang[b] and Hongsik Byun *[b]

In this article, polyketone (PK) micro/nano fiber membranes were successfully fabricated by electrospinning and a post treatment process and the membrane characteristics were investigated. The morphology of the fiber membranes showed that ambient humidity during electrospinning changed the roughness of the fiber surface and the addition of NaCl decreased the fiber diameter. In particular, the changes in surface roughness was a very rare and novel discovery. The effect of this discovery on membrane properties was also analyzed. Additionally, the nanofiber membrane was modified by *in situ* surface reduction. FT-IR spectroscopy indicated the successful reduction modification and water contact angle results proved the improved wetting ability by this modification process. DSC and TGA analysis showed that the micro/nano fiber membranes possessed a high melting point and thermal decomposition temperature. Mechanical tests showed that as fiber membranes, PK micro/nano fiber membranes had relatively high mechanical strength, furthermore the mechanical strength can be easily enhanced by controlling the fiber morphology. From these results, it was concluded that the PK micro/nano fiber membranes could be a promising candidate for many applications such as organic solvent-resistant membranes, high-safety battery separators, oil–water separation, *etc.*

Received 23rd September 2020
Accepted 9th December 2020

DOI: 10.1039/d0ra08119a

rsc.li/rsc-advances

Introduction

Micro/nano fibers can be manufactured from a wide range of polymer materials and several methods have been introduced to fabricate micro/nano fibers, such as template, self-assembly, phase separation, melt-blown and electrospinning. Electrospinning is a relatively simple, versatile process and generally considered the most promising technique to manufacture continuous micro/nano fibers on a large scale.[1–6] As reported in the previous literature, four key parameters can affect the electrospinning process which can be classified into system, solution, process and ambient parameters.[7,8] These electrospun fibers have extremely high specific surface area due to their thin diameters, and these fiber mats can be greatly porous with excellent pore interconnection. Hence, it can be used in the applications where high surface area-to-volume or length-to-diameter ratios are required.[9–11] Moreover, the diameter can be simply adjusted from micrometers to nanometers by changing the process parameters (applied voltage or distance between tip and collector) or increasing the solution electrical conductivity by adding ionic salts such as KH_2PO_4, NaH_2PO_4 and NaCl into the polymer solution and the pore size can also be easily controlled by commanding the duration time of electrospinning.[7,12–15] These excellent properties of electrospun fibers make them very useful in a wide range of advances applications such as filtrations, affinity membranes and recovery of metal ions, battery separators, tissue engineering scaffolds, wound healing, release control, catalyst and enzyme carriers, sensors, and energy storage so that new applications are still being explored.[16–19,36,37] However, electrospun fibers have relatively weak mechanical properties. In order to address these issues, mechanical properties can be enhanced by using polymeric materials with high mechanical strength, integration various nanofillers such as graphene oxide into the polymeric materials or through a post-treatment process.[20–23]

Aliphatic polyketone is a new ecofriendly thermoplastic polymeric material consisting of a perfectly alternating sequence of ethylene and carbon monoxide, usually regarded as a homopolymer of the repeat unit of $CH_2CH_2C{=}O$. It has a high crystalline melting point (about 220 °C), high gas barrier property, excellent flame retardant, high tenacity, excellent mechanical strength, and excellent chemical resistance. Because of these unique characteristics, ployketone materials have been successfully applied in various fields, such as automotive fuel systems, outer components, electronics, gears, barrier pipes, fibers and films.[24–26] And recently, polyketone has being supposed to be very suitable for organic solvent-resistant

[a]*Department of Chemical Engineering, Zibo Vocational Institute, Zibo, 255314, China*
[b]*Department of Chemical Engineering, Keimyung University, Daegu, 42601, South Korea. E-mail: hsbyun@kmu.ac.kr*

† Electronic supplementary information (ESI) available. See DOI: 10.1039/d0ra08119a

‡ Jian Hou and Chanju Park have contributed equally to this work.

membrane or oil–water separation membrane applications and related studies have been becoming a very hot topic for scientists in this field. Although several lectures and achievements have been reported, the polyketone membranes are still all fabricated by non-solvent induced phase separation (NIPS) process. However, this type of membranes is generally asymmetric structures with high tortuosity that impede rapid permeation resulting in inefficient separation.[27,28] In this work combining advantages of micro/nano fibers and polyketone materials, various types of polyketone microfiber and nanofiber membranes were successfully fabricated *via* electrospinning and post treatment process for the first time. Subsequently, in order to further explore their potential applications, these membranes were characterized by scanning electron microscope (SEM), Fourier transform infrared spectroscopy (FT-IR), water contact angle (WCA), differential scanning calorimetry (DSC), thermogravimetric analysis (TGA) and mechanical test.

Experimental section

Materials

Polyketone (PK, MW = 180 000 g mol^{-1}; T_g and T_m are 10 °C and 220 °C) was kindly supplied by Hyosung corporation (Republic of Korea). Hexafluoro-2-propanol (HFIP) and methyl alcohol (methanol) were used as the solvent of electrospinning solution and were purchased by Daejung Chemicals & Metals Co., Ltd. (Republic of Korea). Sodium borohydride ($NaBH_4$) was used in the *in situ* surface reduction of nanofiber membranes and was purchased by Daejung Chemicals & Metals Co., Ltd. (Republic of Korea). Sodium chloride (NaCl) was used as an additive in the electrospinning nanofiber solutions and was purchased by Duksan Pure Chemical Co., Ltd. (Republic of Korea). All chemicals were used as received without further purification.

Fabrication of polyketone (PK) micro/nano fiber membranes

The PK micro/nano fiber membranes were manufactured by the electrospinning process and post treatment process which is showed in Fig. 1. The electrospinning process involved in two steps; the first step was the preparation of the electrospinning solutions by mixing PK pellet and HFIP as solvent. The composition of the solution is listed in Table 1. The second step involved the optimization of the electrospinning solution under various conditions. The prepared solutions were transferred to a 5 mL syringe and then the syringe was positioned vertically for at least 30 minutes to remove the air bubbles completely before electrospinning starts. In this electrospinning system, the ejection speed was controlled by an automated syringe pump (KDS100, KD Scientific Inc.), and the voltage supply equipment used was a CPS 60K02VIT (Chungpa EMT Co., Ltd.). The ambient humidity was controlled by a humidifier. Finally, in order to produce the nanofiber membranes, we changed the applied voltage, used a thinner needle and added an additive (NaCl) to obtain higher conductivity of the electrospinning solution, resulting in an improved spinnability and thereby a thinner diameter of the fibers. All the prepared electrospinning precursor solutions were subjected to electrospinning

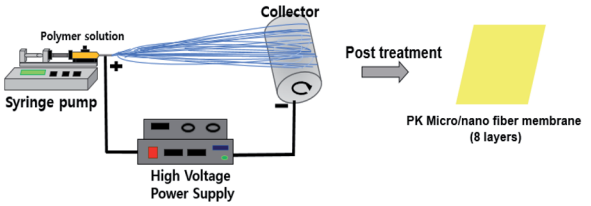

Fig. 1 Schematic illustration of the manufacturing PK micro/nano fiber membrane.

at room temperature under various conditions and the optimized conditions were shown in Table 2. The resulting micro/nano fibers were then dried at 40 °C in a vacuum oven for 24 h to remove the remaining solvent completely. After folding these fibers into 8 layers, the pressure (room temperature, 5000 psi) was lightly applied for 5 s to form the PK membranes. Additionally, the PK nanofiber membrane modified by a simple *in situ* surface reduction using $NaBH_4$. The nanofiber membrane was immersed in a 0.5 wt% $NaBH_4$ aqueous solution for several minutes, and then washing in water, acetone, and hexane in sequence, and then dried in air. And the influence of reduction modification on membrane properties was further studied simultaneously.

Characterizations of polyketone (PK) micro/nano fiber membranes

The morphology of the PK micro/nano fiber membranes was examined by scanning electron microscope (SEM; JSM5410, Jeol) after coating with a gold target. The fiber diameters and diameter distributions were calculated by the image analyzer (I-solution, IMTechnology Inc.). The conductivities of the electrospinning solutions were calculated by following equation:

$$\sigma = \frac{L}{A \times R}$$

where σ is the conductivity of electrospinning solution (μS cm^{-1}), L is the distance between two aluminium flat plates (cm), A is the area of aluminium flat plate (cm^2) and R is the resistance of electrospinning solution (MΩ). The resistance was measured by the digital multimeter (JT-6, Protek). The two aluminium flat plates wired with a digital multimeter were placed in electrospinning solution that poured in vessel. The distance and area of two aluminium flat plates were 1.5 cm and 0.49 cm^2, respectively.

The thickness of membranes was estimated by a digital thickness gage (ABS Digimatic Thickness Gauge, Mitutoyo

Table 1 Composition of polyketone electrospinning solutions (LH: low humidity (30%); HH: high humidity (70%))

Sample name	PK (g)	HFIP (g)	Methanol (g)	NaCl (g)
PK-LH	0.88	10.12	—	—
PK-HH	0.88	10.12	—	—
PK-NaCl	0.711	7.452	0.828	0.009

Table 2 Electrospinning conditions of corresponding polyketone solutions

Sample name	Voltage (kV)	Flow rate (mL h^{-1})	TCD (cm)	Duration (h)	Relative humidity (%)	Syringe tip (gauge)
PK-LH	6	0.8	15	6	30	26
PK-HH	6	0.8	15	6	70	26
PK-NaCl	13	0.8	15	6	30	30

Corp.). The pore size properties of the membranes were analyzed with a capillary porometer (Porolux 1000, IB-FT GmbH) under wet and dry conditions by using a Porewick standard solution with a 16.0 dynes cm^{-1} surface tension. The porosity of the samples (40 mm × 40 mm) was evaluated by comparing the dry and wet weights of the membranes after fully immersing in *n*-butanol for 1 h. The chemical compositions of polyketone membranes were analyzed by Fourier-transform infrared spectroscopy (FTIR; iS50 FT-IR, Thermo Fisher Scientific) with attenuated total reflectance mode. The water contact angles (WCA) of the samples were characterized by a contact angle tester equipped with a digital camera (Phoenix 300, SEO Inc). The differential scanning calorimeter (DSC; DSC25, TA Instruments, USA) and thermogravimetric analysis (TGA; TGAN-1000, Scinco) were used to examine the thermal stability of the membranes. DSC and TGA curves were recorded under N_2 gas at a heating rate of 10 °C min^{-1} from 25 to 250 °C and 25 to 800 °C, respectively. The mechanical properties were measured with a universal tensometer (Tensometer 2020, Myungji Tech) under a tensile speed of 500 mm min^{-1} after clamped the sample on both clamps by 10 mm with the sample size of 80 mm × 20 mm.

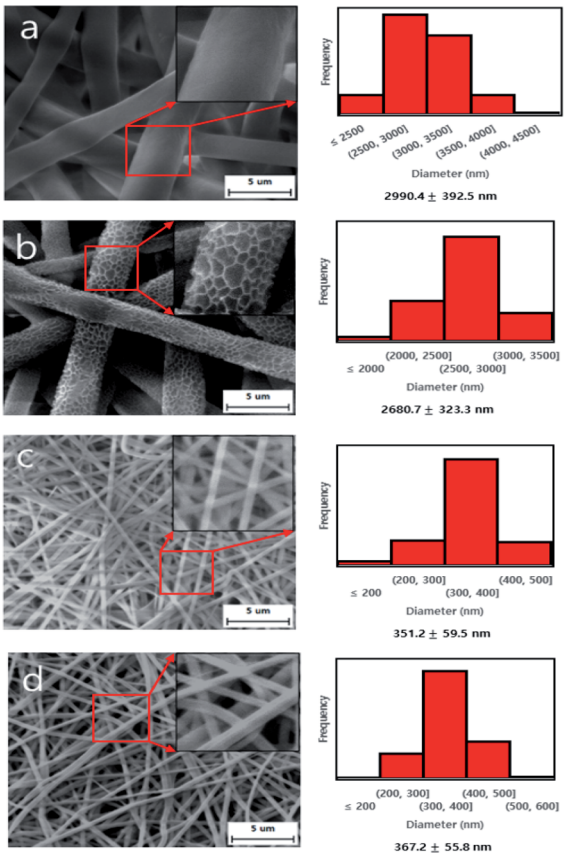

Fig. 2 SEM images (×5000) with zoomed images (×10 000) and diameter distributions of PK micro/nano fiber membranes; (a) PK-LH, (b) PK-HH, (c) PK-NaCl, (d) rPK-NaCl.

Results and discussion

The SEM image and diameter distributions of the electrospun PK micro/nano fiber membranes are shown in Fig. 2. It can be found in Fig. 2a and b that the microfiber produced under low humidity has a smooth surface, while the microfiber produced under high humidity has a rough surface. This surface change was caused by the rapid phase inversion between the volatile solvent (HFIP) and water molecules. In other words, during this electrospinning process, if the surrounding humidity is high, the water molecules will promote mutual transformation as the HFIP evaporates, resulting in the formation of rough surface fibers.[29,35] This is a very rare and novel discovery in the field of fiber mat membranes, and it may affect the characteristics of membranes. The average diameters of the PK fiber membranes dramatically decreased from ~3000 nm (microfiber) to ~350 nm (nanofiber) due to both the addition of NaCl and applied voltage increasing. Table 3 showed the conductivity of the corresponding electrospinning solutions and it was revealed that the conductivity of electrospinning solution played an important role to determine the size of fiber. As the conductivity of electrospinning solution increased the nanofiber size decreased with uniform nanofiber due to the increased elongation force of nanofiber caused by the high charge density.[7,14] As shown in Table 4, the pore size and porosity of the microfiber membrane produced under high humidity were significantly smaller than that of the microfiber membrane produced under low humidity. This can be explained by the microfibers with a rough surface, which will be interlocked with each other like a gear during the post treatment process. Due to the higher

Table 3 Conductivity of the corresponding electrospinning solutions

Sample name	Resistance (MΩ)	Conductivity (μS cm^{-1})
PK-LH	11.5	0.266
PK-NaCl	2.9	1.056

Table 4 Pore size, porosity and water contact angle of PK micro/nano fiber membranes

Sample name	Biggest pore size (μm)	Smallest pore size (μm)	Average pore size (μm)	Thickness (μm)	Porosity (%)	Water contact angle (°)
PK-LH (microfiber)	5.53	2.89	3.65	90 ± 2	82.22 ± 2	60 ± 3
PK-HH (microfiber)	3.16	1.43	1.67	88 ± 3	61.10 ± 2	95 ± 2
PK-NaCl (nanofiber)	0.427	0.207	0.231	105 ± 2	79.76 ± 2	48 ± 2
rPK-NaCl (nanofiber)	0.603	0.290	0.329	126 ± 3	77.61 ± 3	10 ± 2

specific surface of nanofibers, for the same 8-layer membranes the thickness of the nanofiber membranes was obviously increased compared with the microfiber membranes.[10,11] It was also found that the reduction process affected the thickness of PK-NaCl. This might be occurred by the small portion of swelling during the reduction process since the PK-NaCl was very hydrophilic, resulting in the small increase of thickness.

Fig. 3 showed the FT-IR spectra of PK membranes. The strong carbonyl bands (C=O) were showed at 1690 cm^{-1}. The ketone groups of PK-NaCl nanofiber membrane can be converted to hydroxyl groups using $NaBH_4$ and the broad hydroxyl band (–OH) at 3200–3600 cm^{-1} in Fig. 3d confirms the successful conversion after the reduction modification.[30–32] This reduced PK-NaCl nanofiber membrane was defined as rPK-NaCl. The contact angle of the PK-LH microfiber membrane, the PK-HH microfiber membrane, the PK-NaCl nanofiber membrane and the rPK-NaCl nanofiber membrane were given in Table 4 and Fig. 4. The PK-LH microfiber membrane had a hydrophilic contact angle of ~60° and the PK-HH microfiber membrane demonstrated a hydrophobicity with a measured contact angle of ~95°. We predicted that the rough surface may prevent water drop from passing through the membrane, resulting in the PK-HH sample showed a high contact angle. However, when we prepared nanofiber with PK-NaCl the hydrophilic property increased, due to the both the nano size of fiber resulting in the low surface tension of water droplet and the hydrophilic NaCl groups in PK. In Fig. 4c and d, it can be found that the reduction modification nanofiber membrane (rPK-NaCl) displays a superhydrophilicity (~10°). This is because of the *in situ* surface reduction modification will convert partial ketone groups at the membrane surface to more hydrophilic hydroxyl groups.

To analyze the melting behavior of PK membranes, thermal analysis by DSC was conducted, as shown in Fig. 5a. The melting point (T_m) of all types of membranes are almost same,

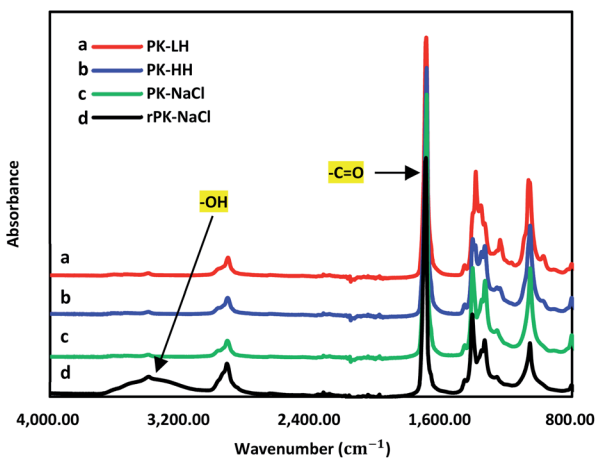

Fig. 3 FT-IR of PK micro/nanofiber membranes.

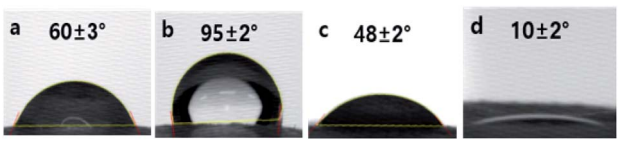

Fig. 4 Contact angle of PK micro/nano fiber membranes; (a) PK-LH, (b) PK-HH, (c) PK-NaCl, (d) rPK-NaCl.

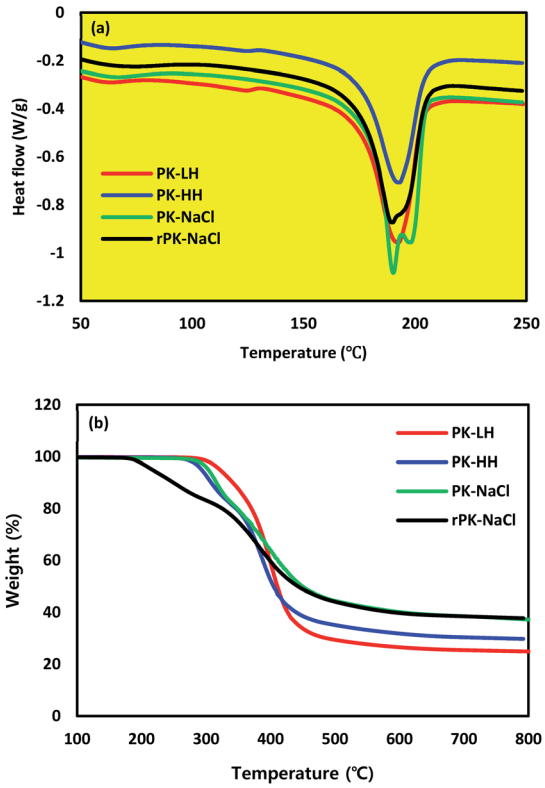

Fig. 5 Thermal analysis of PK micro/nano fiber membranes; (a) DSC curves of different PK micro/nano fiber membranes, (b) TGA curves of different PK micro/nano fiber membranes.

Table 5 Thermal properties of PK, PE, PP and PAN membranes (IDT: initial decomposition temperature, FDT: final decomposition temperature)[19,33,34]

Sample name	Melting point (°C)	IDT (°C)	FDT (°C)
PK-NaCl	200	300	500
PAN	300	305	480
PE	140	450	500
PP	167	400	475

ranging from 190 °C to 200 °C, which implies that there are no defects in changing the fiber diameter size and reduction process. As shown in Fig. 5b, TGA analysis was conducted to observe the thermal properties of the PK membranes. All types of PK membranes showed a weight loss at ~300 °C, corresponding to the decomposition temperature. However, the rPK nanofiber membrane clearly showed a weight loss at ~200 °C, which implied the conversion of ketone groups to hydroxyl groups after reduction. Table 5 showed the thermal property of PK compared with the other membranes such as PAN nanofiber membrane for water treatment application and PE or PP membranes for Li-ion battery application.[33,34] As a result, PK showed the similar thermal property with PAN, indicating there might be no problem at high temperature water treatment application. However, Table 5 indicated that PK had better thermal property than the commercial PE or PP battery separators.[34] This is very important point that PK can be a usable alternative for the high stable separator at elevated temperature, which is able to prevent from the thermal shrinkage during the high charge rate.[19]

Fig. 6 and Table 6 show the stress–stain curves of all types of micro/nano fiber membranes and tensile strength and elongation of micro/nano fiber membranes, respectively. Both nanofiber membranes (Fig. 6c and d) exhibited a much higher tensile strength than the microfiber membranes due to the larger specific surface area, the more irregular pore structure of nanofiber mats and the dense packing of nanofiber layers. While, both microfiber membranes (Fig. 6a and b) showed much higher extension than the nanofiber membranes due to their thicker diameter than nanofiber membranes. And an additional interesting finding was that the tensile strength of PK-HH microfiber membrane was improved very obviously than the PK-LH microfiber membrane. This was owing to the rough surface of the microfibers which was shown in SEM image of Fig. 2b and the inter-fiber interlocking among them.

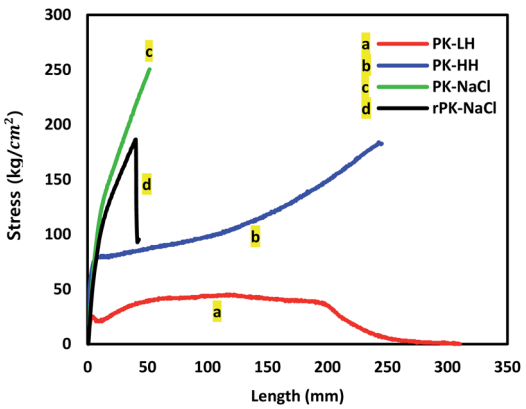

Fig. 6 Tensile strength of PK micro/nano fiber membranes.

Table 6 Tensile strength and elongation of PK micro/nano fiber membranes

Sample name	Tensile strength (kg cm^{-2})	Elongation (%)
PK-LH	45.5	518.3
PK-HH	183.3	409.6
PK-NaCl	250.5	86.2
rPK-NaCl	186.3	71.2

Conclusions

To the best of our knowledge, in this study the PK micro/nano fiber membranes were successfully prepared by electrospinning and post treatment process for the first time. The prepared PK micro/nano fiber membranes were characterized by SEM, pore property, FT-IR, contact angle, thermal stability, physical property, *etc.* An interesting finding was that the morphology and roughness of the fiber membranes could be facilely controlled, and this could take a huge impact on the performance of membranes especially in pore property, surface hydrophilicity and mechanical property. Overall, all the types of the PK micro/nanofiber membranes in this work presented adjustable pore size, high porosity, controllable surface hydrophilicity, excellent thermal stability and enhanced mechanical properties, and these results can make the PK micro/nano fiber membranes as a potential candidate for various future applications, including organic solvent-resistant membrane, thermal-stable (high-safety) battery separators, high efficiency oil–water separation, *etc.* And the further research about these applications are being investigated.

Conflicts of interest

There are no conflicts to declare.

Acknowledgements

We gratefully acknowledge the support from the Department of Chemical Engineering of Zibo Vocational Institute and the College of Engineering of Keimyung University. This research is supported by the Technology Transfer and Commercialization Program through INNOPOLIS Foundation funded by the Ministry of Science and ICT (2019-DG-RD-0004). And this work is also supported by the National Research Foundation of Korea Grant funded by the Korean Government (NRF 2018R1A2B6008854).

References

1 J. Hou, J. Yun and H. Byun, *Membranes*, 2019, **9**, 122–131.
2 J. Shayapat, O. H. Chung and J. S. Park, *Electrochim. Acta*, 2015, **170**, 110–121.
3 A. Abdelrasoul, H. Doan, A. Lohi and C. H. Cheng, *ChemBioEng Rev.*, 2015, **2**, 22–43.
4 P. Arribas, M. Khayet, M. García-Payo and L. Gil, *Sep. Purif. Technol.*, 2014, **138**, 118–129.
5 J. F. Kim, J. H. Kim, Y. M. Lee and E. Drioli, *AIChE J.*, 2016, **62**, 461–490.
6 P. Raghavan, D. H. Lim, J. H. Ahn, C. Nah, D. C. Sherrington, H. S. Ryu and H. J. Ahn, *React. Funct. Polym.*, 2012, **72**, 915–930.
7 X. Tan and D. Rodrigue, *Polymers*, 2019, **11**, 1160–1198.
8 N. Bhardwaj and S. C. Kundu, *Biotechnol. Adv.*, 2010, **28**, 325–347.
9 J. Fang, H. Niu, T. Lin and X. Wang, *Chin. Sci. Bull.*, 2008, **53**, 2265–2286.
10 S. Homaeigohar and M. Elbahri, *Materials*, 2014, **7**, 1017–1045.
11 X. Wang and B. S. Hsiao, *Curr. Opin. Chem. Eng.*, 2016, **12**, 62–81.
12 X. Yuan, Y. Zhang, C. Dong and J. Sheng, *Polym. Int.*, 2004, **53**, 1704–1710.
13 Y. Yao, P. Zhu, H. Ye, A. Niu, X. Gao and D. Wu, *Front. Chem. China*, 2006, **1**, 334–339.
14 S. J. Kim, C. K. Lee and S. I. Kim, *J. Appl. Polym. Sci.*, 2005, **96**, 1388–1393.
15 X. Zong, K. Kim, D. Fang, S. Ran, B. S. Hsiao and B. Chu, *Polymer*, 2002, **43**, 4403–4412.
16 K. Jayaraman, M. Kotaki, Y. Zhang, X. Mo and S. Ramakrishna, *J. Nanosci. Nanotechnol.*, 2004, **4**, 52–65.
17 Z.-M. Huang, Y.-Z. Zhang, M. Kotaki and S. Ramakrishna, *Compos. Sci. Technol.*, 2003, **63**, 2223–2253.
18 A. L. Yarin, S. Koombhongse and D. H. Reneker, *J. Appl. Phys.*, 2001, **89**, 3018–3026.
19 J. Hou, W. Jang, S. Kim, J.-H. Kim and H. Byun, *RSC Adv.*, 2018, **8**, 14958–14966.
20 H. Lee, M. Yanilmaz, O. Toprakci, K. Fu and X. Zhang, *Energy Environ. Sci.*, 2014, **7**, 3857–3886.
21 W. Jang, J. Yun, K. Jeon and H. Byun, *RSC Adv.*, 2015, **5**, 46711–46717.
22 J. Hou, J. Yun, S. Kim and H. Byun, *Appl. Sci.*, 2019, **9**, 962–966.
23 S.-S. Choi, Y. S. Lee, C. W. Joo, S. G. Lee, J. K. Park and K.-S. Han, *Electrochim. Acta*, 2004, **50**, 339–343.
24 J. M. Lagaron, A. K. Powell and N. S. Davidson, *Macromolecules*, 2000, **33**, 1030–1035.
25 P. Gupta, J. Schulte, J. Flood and J. Spruiell, *J. Appl. Polym. Sci.*, 2001, **82**, 1794–1815.
26 O. Ohsawa, K.-H. Lee, B.-S. Kim, S. Lee and I.-S. Kim, *Polymer*, 2010, **51**, 2007–2012.
27 L. Zhang, L. Cheng, H. Wu, T. Yoshioka and H. Matsuyama, *J. Mater. Chem. A*, 2018, **6**, 24641–24650.
28 C. Liu, R. Takagi, T. Shintani, L. Cheng, K. L. Tung and H. Matsuyama, *ACS Appl. Mater. Interfaces*, 2020, **12**, 7586–7594.
29 M. Bognitzki, W. Czado, T. Frese, A. Schaper, M. Hellwig, M. Steinhart, A. Greiner and J. H. Wendorff, *Adv. Mater.*, 2001, **13**, 70–72.
30 S. Li, Y. Yang, X. Zha, Y. Zhou, W. Yang and M. Yang, *Nanomaterials*, 2018, **8**, 932–947.
31 L. Cheng, D.-M. Wang, A. R. Shaikh, L.-F. Fang, S. Jeon, D. Saeki, L. Zhang, C.-J. Liu and H. Matsuyama, *ACS Appl. Mater. Interfaces*, 2018, **10**, 30860–30870.
32 L. Cheng, A. R. Shaikh, L.-F. Fang, S. Jeon, C.-J. Liu, L. Zhang, H.-C. Wu, D.-M. Wang and H. Matsuyama, *ACS Appl. Mater. Interfaces*, 2018, **10**, 44880–44889.
33 W. Jang, Y. Park, C. Park, Y. Seo, J.-H. Kim, J. Hou and H. Byun, *J. Membr. Sci.*, 2020, **598**, 117670.
34 Y. Li, X. Wang, J. Liang, K. Wu, L. Xu and J. Wang, *Polymers*, 2020, **12**, 764.
35 C. L. Casper, J. S. Stephens, N. G. Tassi, D. B. Chase and J. F. Rabolt, *Macromolecules*, 2004, **37**, 573–578.
36 M. Venkatesan, L. Veeramuthu, F.-C. Liang, W.-C. Chen, C.-J. Cho, C.-W. Chen, J.-Y. Chen, Y. Yan, S.-H. Chang and C.-C. Kuo, *Chem. Eng. J.*, 2020, **397**, 125431.
37 G. Yang, X. Li, Y. He, J. Ma, G. Ni and S. Zhou, *Prog. Polym. Sci.*, 2018, **81**, 80–113.